Electron Hall Effect in Silicon Dioxide

ALVIN M. GOODMAN
RCA Laboratories, Princeton, New Jersey
(Received 19 June 1967)

A new three-electrode Hall-effect geometry has been used to determine an approximate mobility value for electrons photoemitted into the conduction band of thermally grown layers of silicon dioxide. The oxide layers were grown in an air-steam atmosphere at 1100–1150°C and were from 3.5 to 6.6 μ thick. The unusual electrode geometry was used in order to keep the electron drift path in the oxide less than the *Schubweg* (mean drift length before immobilization by deep trapping). The geometry is not easy to analyze, and only approximate analyses have thus far been obtained. The observed effect is in all cases of the correct polarity for electrons, and to a good approximation varies linearly with magnetic field strength. The values of electron mobility obtained from the measurements range from 6.8 to 62.5 cm^2/V-sec with an average value of about 29 cm^2/V-sec.

I. INTRODUCTION

RECENT investigations[1,2] of the electron transport properties of thermally grown layers of silicon dioxide have shown that electrons injected into the oxide conduction band (by photoemission from an adjacent electrode) can be drifted through several microns of oxide without significant trapping. This was accomplished by applying high electric fields ($\sim 10^5 - 10^6$ V/cm) to the oxide layers.

At somewhat lower fields significant electron trapping did occur. This was studied in detail by Williams[1] who found that the deep trap density is $\sim 3\times 10^{14}/cm^3$ and the capture cross section is 1.3×10^{-12} cm^2. By comparing this cross section with a model for capture by a Coulomb attractive center, he was able to estimate a value for the microscopic mobility of electrons in the SiO_2 conduction band. This estimated value is either 34 or 17 cm^2/V-sec, depending upon whether the trapping center is singly or doubly charged.

This relatively high value of electron mobility for a vitreous (noncrystalline) material is rather interesting if not surprising and therefore engendered some thought about alternative measurements of the mobility.

The most usual and most direct method for determination of electron mobility is the Hall-effect measurement.[3] However, the usual Hall-effect geometry would be rather difficult to employ in this case because the mean drift length before trapping (*Schubweg*) of photoinjected electrons in thermally grown SiO_2 layers[2] is $\gtrsim 20\mu$ (at $E = 10^6$V/cm). Therefore, in order to carry out Hall measurements (without excessive electron trapping) a new three-electrode configuration was devised in which the electron drift paths would be less than 20 μ. The new three-electrode geometry is not easy to analyze and only approximate analyses have thus far been effected. Within the limitations of the approximations employed in analyzing the effect and the scatter of experimental data, the results are in good agreement with those of Williams.

[1] R. Williams, Phys. Rev. **140**, A569 (1965).
[2] A. M. Goodman, Phys. Rev. **144**, 588 (1966).
[3] E. H. Putley, *The Hall Effect and Related Phenomena* (Butterworth Scientific Publications, Ltd., London, 1960), Chap. II.

The theory of the measurement is presented in Sec. II; this includes a physical description of the experiment, two approximate analyses of the measurement, and a discussion of the approximations involved. In Sec. III, the experimental details are described. The results of the measurements are presented and discussed in Sec. IV.

II. THEORY

A. Qualitative Description

In the three-terminal Hall-effect measurements, electrons are injected (by photoemission) into a silicon dioxide layer at its interface with the silicon wafer on which it was grown. The electrons are then drifted through the layer to two evaporated metallic counterelectrodes which are equidistant from the photoemitting surface and separated from each other by a distance of the order of magnitude of the layer thickness. A cross-section view of such an arrangement (without magnetic field) is shown in Fig. 1. The metal counterelectrodes are opaque and define the light pattern on the photoemitting silicon surface. If the potentials applied to the counterelectrodes are equal and the incoming light is of normal incidence, the circuit is balanced and the electron paths follow the electric field

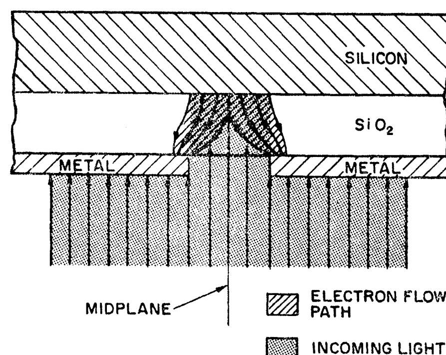

FIG. 1. Qualitative sketch of electron paths through the SiO. layer with no applied magnetic field. When the magnetic field is applied (during the Hall-effect measurement), it is normal to the plane of the figure.

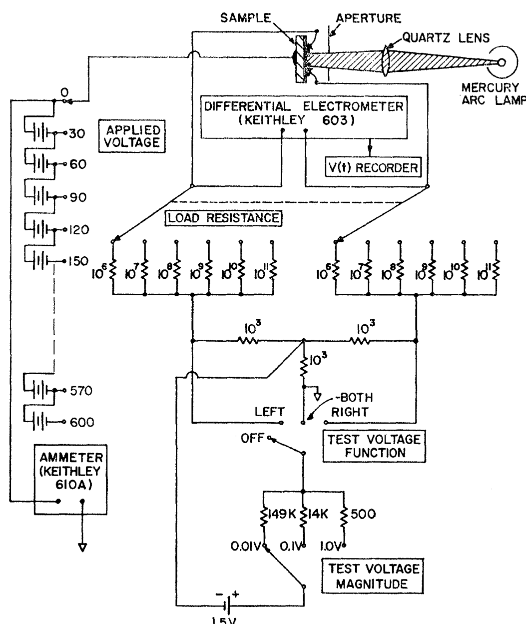

FIG. 2. Schematic circuit diagram for three terminal Hall-effect measurement.

lines as shown qualitatively in Fig. 1. If a magnetic field is applied (perpendicular to the plane of the figure), the electron paths will be altered and the currents to the two counterelectrodes will no longer be balanced, or alternatively, a difference of potential between the two counterelectrodes will be required to maintain the current balance which existed before the magnetic field was turned on. In parts B and C of this section, the effect of the magnetic field is quantitatively related to the mobility.

B. Hall-Effect "Voltage Analysis"

1. *Circuit Analysis*

(*a*) *Measurement circuit.* The actual measurement circuit is shown in Fig. 2. A voltage V is applied between the silicon wafer and ground. The evaporated metal counterelectrodes are connected through a pair of matched load resistors to ground. A differential electrometer is used to measure the voltage developed between the counterelectrodes. The test voltage function

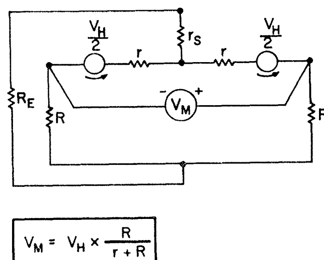

FIG. 3. Simplified equivalent circuit with magnetic field on and test voltage off.

switch may be used to insert 0.01, 0.1, or 1.0 V in series with either load resistor (or in series with both of them with reversed polarity).

The simplified equivalent circuit with magnetic field on and test voltage off is shown in Fig. 3. The sample is represented by the two equivalent Hall generators, each producing an open circuit voltage $V_H/2$ and having a series resistance r. The other resistances in the circuit are: r_s, an additional sample resistance; R_E, the electrometer resistance; and the two load resistors each having a resistance R. It is easily verified that the voltage read at the differential electrometer V_M is related to the Hall voltage V_H by

$$V_M = V_H R/(r+R). \tag{1}$$

Note that this relation is independent of r_s and R_E.

(*b*) *Test circuit.* The value of the "sample arm" resistance r may be determined by inserting a test voltage V_T in series with one of the load resistors and measuring the resultant shift in the differential electrometer voltage V_{MT}. This is shown in Fig. 4. It is easily shown that

$$r = R/[(V_T/V_{MT})-1]. \tag{2}$$

Note that Eq. (2) is independent of r_s and R_E.

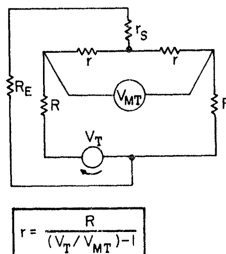

FIG. 4. Simplified equivalent circuit with test voltage V_T on and magnetic field off.

2. *Uniform Field Approximation*

The electric field configuration in the SiO_2 is difficult to determine for the general case of arbitrary values of t (thickness of the oxide layer) and w (gap width between the counterelectrodes). In order to obtain an approximate solution to the problem, a simplified model with an obviously fictitious uniform field distribution has been adopted. In Fig. 5, the path *bac* is considered to obtain the Hall voltage V_H. The average value of the electric field along the path *ba* (and along the path *ca*) is

$$\bar{E} = V/[t^2+(w/2)^2]^{1/2}, \tag{3}$$

where V is the applied voltage. The average component in a direction normal to the silicon surface is

$$\bar{E}_N = \bar{E}t/[t^2+(w/2)^2]^{1/2} = Vt/[t^2+(w/2)^2]. \tag{4}$$

The resultant average Hall field is

$$\bar{E}_H = \bar{v}_N B = \mu \bar{E}_N B, \tag{5}$$

where $\bar{v}_N$ is the average electron drift velocity component in a direction normal to the silicon surface, μ

is the electron mobility, and B is the magnetic flux density. The Hall voltage is

$$V_H = \bar{E}_H w = \{w\mu VB/t[1+(w/2t)^2]\}. \quad (6)$$

By combining Eqs. (1) and (6) one obtains

$$\mu_V = [(R+r)/r][V_M/VB][\{t/w\}\{1+(w/2t)^2\}], \quad (7)$$

where the value of the mobility obtained from this analysis has been labeled μ_V to differentiate it from the mobility obtained from the "current analysis" in part C of this section. The dependence of Eq. (7) on the sample geometry is contained in the last factor in the square brackets. The dependence of that factor on the ratio (t/w) is shown in Fig. 6.

C. Hall-Effect "Current Analysis"

If the two counterelectrodes are kept at the same potential when the magnetic field is turned on, the current flow pattern should change, and a resultant differential current should then pass through the load resistors in the measurement circuit. In analyzing the effect, the following statements are assumed to be true.

(i) Transverse E on the midplane is zero (See Fig. 1).

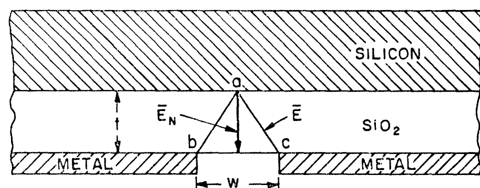

FIG. 5. Simplified model used for the uniform-field approximation in the Hall-effect "voltage analysis."

(ii) Transverse E close to the midplane is small enough to be neglected and the only transverse force on the electrons is the Lorentz Force.

(iii) The emitted current density J of electrons per unit width of the emitting surface is I/w, where I is the total current.

These assumptions are equivalent to analyzing the geometry shown in Fig. 7 in which the mathematical spacing between the counterelectrodes is reduced to zero. The Hall current ("short circuit current" due to the magnetic field) is

$$I_H = Jt\tan\theta, \quad (8)$$

where θ is the Hall angle and is equal to μB. The voltage observed at the differential electrometer is

$$V_M = 2RIt[\tan(\mu B)]/w. \quad (9)$$

If $\theta \ll 1$, then the mobility obtained from the "current analysis" is

$$\mu_I = V_M w/2RItB. \quad (10)$$

It should be noted that, strictly speaking, there is a difference between the definitions of μ_V and μ_I. In the

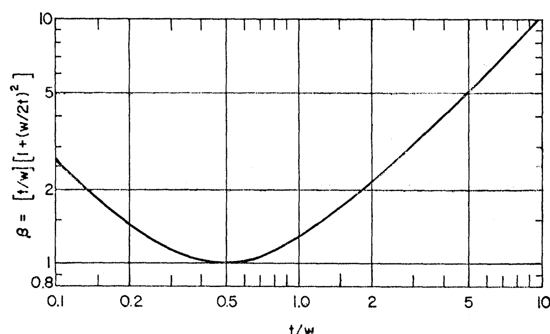

FIG. 6. Dependence of the sample geometry factor in Eq. (7) on the ratio of thickness t to gap width w.

"voltage analysis," μ_V was defined as a ratio of drift velocity to electric field, i.e., as a *drift mobility*. However, in the "current analysis," μ_I was introduced as a *Hall mobility* ($\mu_I B$ = Hall angle). If one assumes that conduction occurs by the conventional band and scattering mechanisms, the ratio of the two mobilities would be expected to differ at most by a numerical factor of order unity,[3] and hence be of little consequence. However, differences due to shallow trapping or to the possibility of narrow-band or hopping-type conduction would require further study. It will be seen in Sec. IV that the latter possibility is almost certainly ruled out by the magnitude of the experimentally determined mobility. In any case, a full discussion of this subject is beyond the scope of the present work.

III. EXPERIMENTAL DETAILS

A. Sample Preparation

The oxide films were grown on the (111) faces of single-crystal degenerate silicon wafers. The growth was carried out in an air-steam atmosphere at either 1100 or 1150°C depending upon the wafer. In all, four oxide layers (on four separate wafers) were used. A (low-resistance) pressure contact to the back of each silicon wafer was obtained by sand-blasting that surface to remove the oxide.

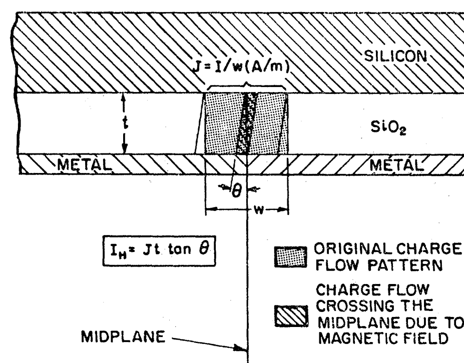

FIG. 7. Simplified model used for the Hall-effect "current analysis" The magnetic field is normal to the plane of the figure.

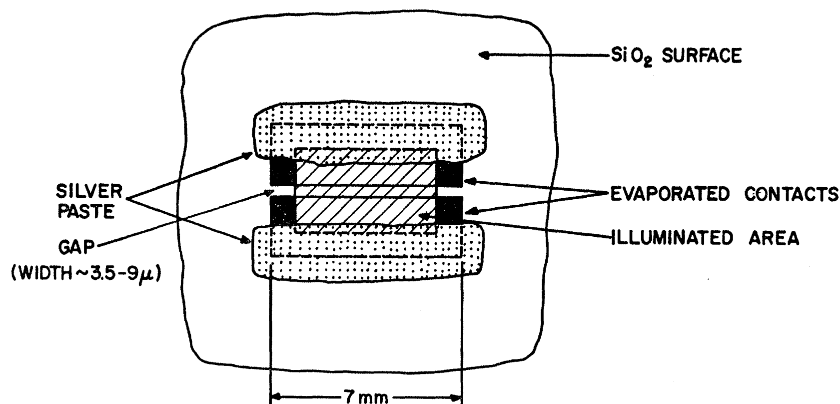

FIG. 8. Enlarged top surface schematic view of a portion of a sample prepared for measurement (not to scale).

The required counterelectrode structures were produced by two different techniques: (1) evaporation through a mask and (2) photolithography. The gap length in each case was about 7 mm and the gap width varied between 3.5 and 9 μ as shown in Fig. 8.

1. *Evaporation through a Mask*

Pairs of opaque metallic counterelectrodes were evaporated onto the front face of each oxide layer. A gap between the electrodes was produced by evaporating "around" a thin ($\sim$5–10 μ-diam) tungsten wire stretched across and welded to a metal-foil evaporation mask. Although the wire was in contact with the oxide during the evaporation, the gaps obtained using this technique were not entirely satisfactory. When gold was used as the counterelectrode material it was found that the gap was somewhat narrower than the diameter of the tungsten wire although the evaporation throw distance was about 8 inches and the penumbra effect should have been small. In addition, there were "shorts" across the gaps between adjacent counterelectrodes. These were burned out by placing 100–200 V between the shorted electrodes. The "burning out" or "arcing" of the shorts left irregular gaps as shown in Fig. 9. In most cases the arcing was slight as shown in Fig. 9(a) but in some cases the arcing was quite extensive as shown in Fig. 9(b). Measurements made on samples with extensive arcing were considered unreliable and were therefore discarded. In order to prevent gap shorts, chromium was tried as the counterelectrode metal since the surface mobility of freshly deposited chromium on silicon dioxide is much lower than that of gold.[4] This completely eliminated the short circuits; however, the gap width was still found to be less than the diameter of the wire used as the gap mask.

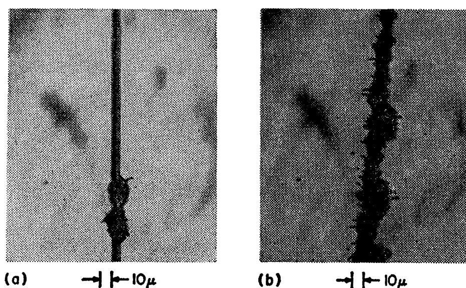

FIG. 9. Photomicrographs of the results of arcing across the gap between evaporated gold counterelectrodes on a Hall sample: (a) slight arcing, (b) extensive arcing.

2. *Photolithographic Technique*

A layer of aluminum about 5000 Å thick was evaporated onto the free surface of the oxide. A glass mask with the desired pattern[5] was used to define the electrodes using Kodak photoresist (KPR)[6] and standard photolithographic methods.[7] A considerable amount of trial and error was required to produce usable gaps by this technique. A typical usable gap obtained in this manner is shown in Fig. 10. Some of the defects which made counter electrodes unusable were (a) uneven etching along the gap, (b) short circuits at various spots along the gap, (c) lateral etching under the resist which caused the gaps to be considerably wider than the corresponding photomask pattern, and (d) pinholes in the counterelectrodes.

After the counterelectrodes were formed (by either technique) they were partially coated with silver paste

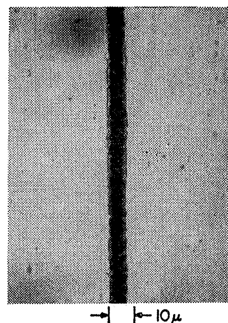

FIG. 10. Photomicrograph of a gap between aluminum counterelectrodes obtained by photolithography.

[4] Nancy Scott Amick, RCA Internal Report (unpublished).
[5] Obtained from Towne Laboratories, Somerville, New Jersey.
[6] Obtained from Eastman Kodak Company, Rochester, New York.
[7] *An Introduction to Photofabrication Using Kodak Photosensitive Resists* (Eastman Kodak Company, Rochester, New York, 1966).

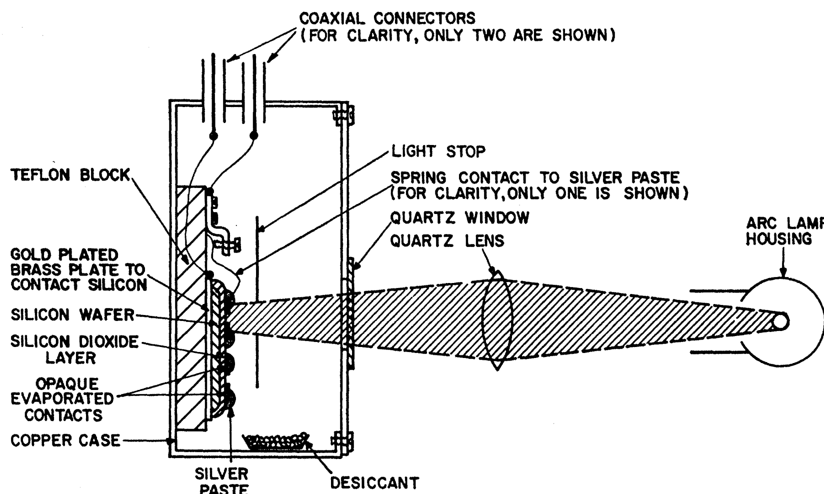

FIG. 11. Cross-section schematic drawing of experimental arrangement. The magnetic field is normal to plane of the figure.

around the edges away from the gap as shown in Fig. 8. The purpose of the silver paste was to provide an opaque, physically tough, conducting surface which would not be penetrated or scraped off by a pressure contact.

B. Experimental Arrangement

A cross-section schematic drawing of the experimental arrangement is shown in Fig. 11. Some of the details in the figure require further explanation: The arc lamp (General Electric H85A3/UV with outer jacket removed) housing contains a mu metal shield to isolate the arc from the fringing field of the magnet. The angle of incidence of the incoming light was adjusted during operation to provide balanced photocurrents to the two counterelectrodes with no applied magnetic field. The desiccant was required to eliminate surface currents on the oxide due to adsorbed moisture. The light stop was used to limit the illumination pattern on the sample to that shown in Fig. 8.

Another point worth mentioning is that it was found necessary to operate the electrometers at some distance from the magnet in order to prevent spurious measurements.

IV. RESULTS AND DISCUSSION

A Hall effect is observed, and the sign is in all cases correct for electrons. A typical recorder plot of the observed Hall voltage is shown in Fig. 12. To a good approximation, the effect in most cases varies linearly with the magnetic field. In a few cases the effect saturated in one magnetic field direction. The reason for the saturation is not known. Three examples of the magnetic field dependence of the Hall effect are shown in Fig. 13. The thickness of each oxide used was measured using an interferometric technique; the values were in the range 3.5 to 6.6 μ. The applied voltage was in all cases between 300 and 600 V. Typical values of photocurrent I were in the range 0.6 to 1.2×10^{-10} A. Typical values of sample arm resistance r were in the range

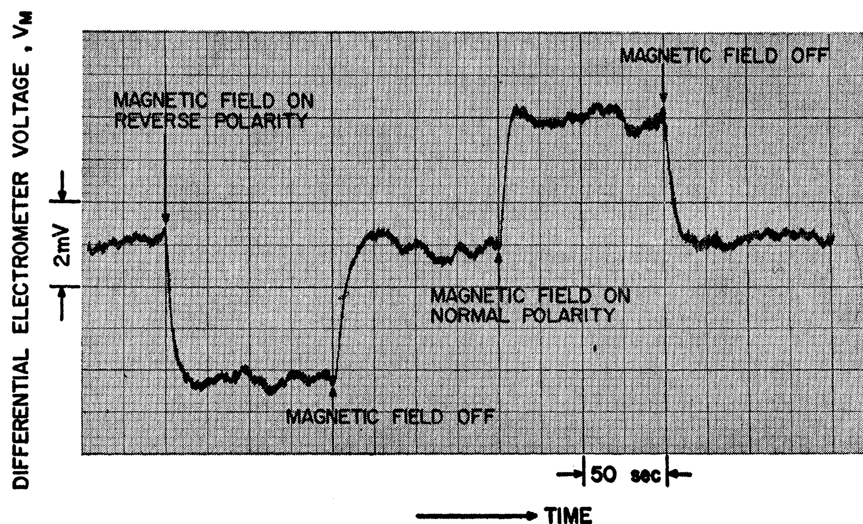

FIG. 12. Recorder plot of observed Hall effect (magnetic field = 10 Wb/m²).

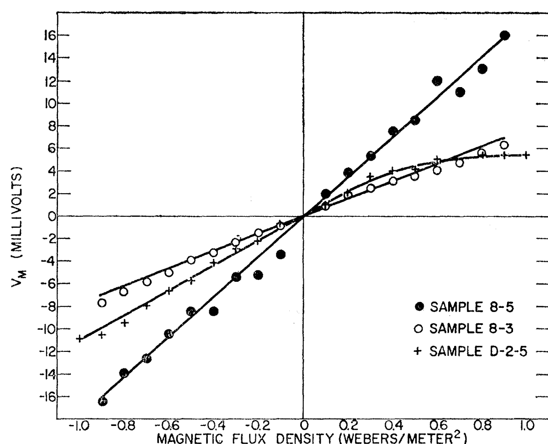

FIG. 13. Magnetic field dependence of the Hall effect for three samples.

$3.5-12.5\times10^{11}$ Ω. Results for 14 sets of electrodes (5 Au, 4 Cr, 5 Al) on four oxide layers range from 7.3 to 62.5 cm²/V-sec for μ_I with an average value, $\bar{\mu}_I=34.4$ cm²/ V-sec. The μ_V values for 11 of these electrode sets (5 Au, 4 Cr, 2 Al) were from 6.8 to 48.4 cm²/V-sec with an average value, $\bar{\mu}_V=23.1$ cm²/V-sec. The value of μ_V could not be calculated for the other three electrode sets because r had not been measured. The average value of $\bar{\mu}_I$ and $\bar{\mu}_V$ is 28.8 cm²/V-sec.

It is worthwhile to consider some of the possible reasons for inaccuracy and scatter in the measured mobility values.

(1) Approximate nature of the analyses. This is probably the principal cause for inaccuracy of the obtained mobility values. An improved (more exact) analysis of the effect would be highly desirable.

(2) Imprecise definition of the gap between the counterelectrodes: The most obvious effect of this is to invalidate (to some extent) the assumption made in the derivation of the expression for μ_I that the photoemitting area of the silicon is uniformly illuminated. If the center region of the photoemitting area were more intensely illuminated than the rest of it, the actual photoemitted current density in the center of the gap would be larger than the apparent value (I/w), leading to an erroneously high value of μ_I. This may be at least a partial explanation for the observation that $\bar{\mu}_I>\bar{\mu}_V$.

(3) Nonuniformity of illumination across the gap. The image of the arc lamp focused on the gap was not entirely uniform and this may have introduced some error. Some indication of the extent of the nonuniformity was obtained in the following way: By scanning the gap across the arc image (the gap is very much smaller than the image) the variation in I was as much as 50% of the maximum value. During the experiment an effort was made to obtain the maximum value of I.

(4) Electron trapping. In spite of the high drift fields and geometry chosen to minimize trapping, some trapping did occur. Typically the photocurrent I decreased 10 to 20% during the time required for measurements using a particular set of electrodes (~30 min). A similar decrease in the differential electrometer voltage V_M (with magnetic field applied) was observed during the same period; thus the effect of electron trapping on the measurement is noticeable but not drastic.

(5) Scatter in measured values. The observed scatter may be at least a partially real effect due to nonuniformity of the oxide layers.

In conclusion, a new three-electrode Hall-effect geometry has been used to determine an approximate mobility value (~29 cm²/V-sec) for electrons in the conduction band of thermally grown layers of silicon dioxide.

ACKNOWLEDGMENTS

It is a pleasure to acknowledge helpful discussions with E. Ramberg, A. Amith, L. R. Friedman, and R. Crandall, and the diligent assistance of J. Breece in the sample preparation and in carrying out the measurements. I also wish to thank N. DiGiuseppe for constructing some of the apparatus, and H. Parker for assistance in sample preparation.

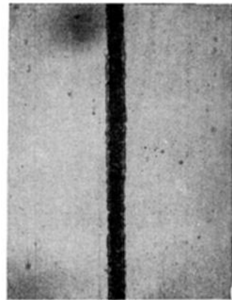

FIG. 10. Photomicrograph of a gap between aluminum counter-electrodes obtained by photolithography.

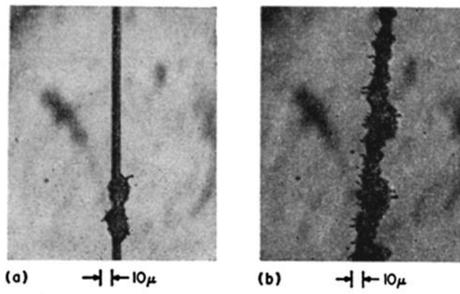

FIG. 9. Photomicrographs of the results of arcing across the gap between evaporated gold counterelectrodes on a Hall sample: (a) slight arcing, (b) extensive arcing.